

ANALYSIS OF EFFECTIVE PARAMETERS FOR SEMBLANCE-BASED COHERENCY ATTRIBUTES TO DETECT MICRO-FAULTS AND FRACTURES

ALI HASHEMI GAZAR¹, ABDOLRAHIM JAVAHERIAN^{2*} and HAMID SABETI³

¹ Institute of Geophysics, University of Tehran, Tehran, Iran. alhashemi@ut.ac.ir

² Institute of Geophysics, University of Tehran, Tehran, Iran.

* present address: Department of Petroleum Engineering, Amirkabir University of Technology, Tehran, Iran. javaheri@ut.ac.ir

³ Birjand University of Technology, Birjand, Iran. hamid.sabeti@gmail.com

(Received October 22, 2009; revised version accepted October 4, 2010)

ABSTRACT

Hashemi Gazar, A., Javaherian, A. and Sabeti, H., 2011. Analysis of effective parameters for semblance-based coherency attributes to detect micro-faults and fractures. *Journal of Seismic Exploration*, 20: 23-44.

Coherency attributes are useful in the interpretation of seismic data and can be applied to 3D seismic data. When coherency attributes are applied to seismic data, they indicate the continuity between two or more traces within a seismic window. The rate of seismic continuity is an index of geological continuity. Areas of traces that change with faults or other geological phenomena have lower coherency in comparison with adjacent traces. Coherency attributes can be divided into three major groups: (1) cross-correlation, (2) eigenstructure and (3) semblance.

In this paper, first, the ability of the three coherency attributes mentioned above to detect micro-faults was tested over 3D real data. The results proved that the semblance algorithm was much more powerful than the other algorithms in detecting micro-faults. Therefore, in the remainder of the study only the semblance attribute was employed. The effect of the dominant frequency, the signal-to-noise ratio, the dimensions of the analysis cube, and the apparent dip in the x- and in the y-directions on the semblance coherency attribute was investigated. The effects of these parameters were tested on 3D synthetic seismic data consisting of (1) horizontal layers, (2) dipping layers, and (3) cross-dipping layers. It is shown that for frequencies up to 20 Hz, there was no clear image of the micro-faults. However, for frequencies above 20 Hz, the resolution of micro-faults was increased. The results indicate that micro-faults are detectable with a signal-to-noise ratio of 1 or higher. When a signal-to-noise ratio of 0.5 is selected, micro-faults can still be detectable but with

a lower resolution. According to synthetic models, a temporal window of 32 ms ($k = 8$) showed the best results for horizontal and dipping layers. The best size for the spatial window is 10×10 for horizontal and dipping layers. Therefore, the optimum cube dimensions of analysis are $10 \times 10 \times 8$. For these dimensions, the signal-to-noise ratio increases and micro-faults are clearly detectable. Regarding the cross-dipping model, apparent dip directions, p and q , were analyzed. The same optimum value of 10 ms/m was obtained for both. Real data which is related to carbonate units showed satisfactory results as well: micro-faults and minor fractures hidden in the primary data were detectable after applying the algorithm.

KEY WORDS: coherency attributes, micro-faults, cross-correlation, eigenstructure, semblance, cross-dipping, 3D seismic data.

INTRODUCTION

Seismic attributes include all the information obtained from seismic data, either by direct measurements or by logical or experience-based reasoning (Taner, 2001). Seismic attributes are very useful in the characterization of faults and fractures on 3D seismic data (Chopra and Marfurt, 2007a). Seismic coherency is a geometrical attribute that establishes temporal and lateral relationships with other attributes. Seismic discoherency denotes a lateral change in seismic response caused by geologic, lithologic, porosity or hydrocarbon existence. The coherency attribute is a mathematical measure of similarity. When it is applied to seismic data, it gives an indication of the continuity between two or more windowed seismic traces (Gersztenkorn and Marfurt, 1999). Coherency attributes are performed on 3D seismic cubes. The first coherency attribute algorithm, called the cross-correlation, was proposed by Bahorich and Farmer (1995) to cross correlate each trace with its in-line and x-line neighbor and then combine the two results after normalizing based on the energy. Since this approach deals with only three traces, it is computationally efficient but lacks robustness, especially when dealing with noisy data. The second generation coherence algorithm (Marfurt et al., 1998) uses a multitrace semblance measure. Using more traces in the coherence computations results in greater stability in the presence of noise. The third generation algorithm is also a multitrace coherence measure. However, it is based on the eigenstructure of the covariance matrix formed from the traces in the analysis cube (Gersztenkorn and Marfurt, 1996a,b; Gersztenkorn et al., 1999). In addition, the eigenstructure algorithm incorporates various filters and interpolation schemes to aid with problems such as poor signal-to-noise ratios and aliasing. These enhancements can often significantly improve the results. Roberts (2001), Hart et al. (2002), Sigismondi and Soldo (2003), and Masafferro et al. (2003) introduced the idea of using the reflection curvature in order to detect fractures. More improvements have been obtained by Al-Dossary and Marfurt (2006) and Chopra and Marfurt (2007b). They used a volume calculation of the reflection curvature to analyze fractures. There are now more than 50 distinct seismic attributes calculated from seismic data and applied in the interpretation of the

geologic structures, stratigraphy, and rock/pore fluid properties (Chopra and Marfurt, 2005). Micro-faults and minor fractures were not studied in these previous works. In this paper the ability of these coherency attributes in detecting the micro-faults are studied, first on the 3D real data, then on 3D synthetic data, consisting of horizontal, dipping and cross-dipping layers. The effects of some parameters on the semblance algorithm are analyzed so that micro-faults and fractures can be detected.

COHERENCY ATTRIBUTES

In attribute classification, the seismic coherency attribute is a branch of geometric attributes. Geometric attributes generally describe the space and instant relationships between all other attributes. Coherency attributes are useful in the interpretation of seismic data and can be applied to 3D seismic data. When coherency attributes are applied to seismic data, they indicate the continuity between two or more traces within a seismic window. The rate of seismic continuity is an index of geological continuity. Areas of traces that change with faults or other geological phenomena have lower coherency in comparison with adjacent traces. These attributes can be divided into three major groups of cross-correlation, semblance-based and eigenstructure coherency algorithms.

Cross-correlation coherency algorithm

The cross-correlation coherency algorithm was developed primarily by Bahorich and Farmer (1995). This algorithm was extended by Marfurt et al (1998) and made it possible to interpret seismic data more precisely. In this approach, to calculate the coherency, three traces are chosen (one as a base and two others in the direction of in-line and x-line). First, coherency is calculated in a finite-time interval along the in-line and, second, along the x-line. Then, the measure of coherency is achieved by multiplying the root of the maximum coherency values in each time interval along in-line and x-line. First, the in-line l-lag cross-correlation is defined as ρ_x at time t between data traces u at positions (x_i, y_i) and (x_{i+1}, y_i) to be

$$\rho_x(t, l, x_i, y_i) = \sum_{\tau=-w}^{+w} u(t-\tau, x_i, y_i) u(t-\tau-l, x_{i+1}, y_i) / \sqrt{\left\{ \sum_{\tau=-w}^{+w} u^2(t-\tau, x_i, y_i) \sum_{\tau=-w}^{+w} u^2(t-\tau-l, x_{i+1}, y_i) \right\}} \quad , \quad (1)$$

where $2w$ is the temporal length of the correlation window (Marfurt et al 1998). Although this algorithm is computationally efficient, it is somewhat limited in dealing with noisy data and this is a disadvantage of the algorithm.

Semblance-based coherency algorithm

The semblance-based coherency algorithm was presented by Marfurt et al. (1998). It is more efficient in comparison with the correlation algorithm. This algorithm starts by defining an elliptical or rectangular analysis window containing a number, J , of traces. The results of the analysis will assign to the center of the window (Fig. 1). Next, the coordinates of this center point (x,y) should be calculated to define the semblance, $\sigma(\tau,p,q)$, by applying the following equation:

$$\sigma(\tau,p,q) = \left[\sum_{j=1}^J u(\tau - px_j - qy_j, x_j, y_j) \right]^2 + \left[\sum_{j=1}^J u^H(\tau - px_j - qy_j, x_j, y_j) \right]^2 \\ / J \sum_{j=1}^J \{ [u(\tau - px_j - qy_j, x_j, y_j)]^2 + [u^H(\tau - px_j - qy_j, x_j, y_j)]^2 \} , \quad (2)$$

where J shows the number of traces, the triple values (τ,p,q) define a local planar event at the time τ , p and q are the apparent dips in the x - and y -directions, respectively, measured in ms/m, and H denotes the Hilbert transform or quadrature component of the real seismic trace u (Marfurt et al., 1998). This method is employed using as narrow a temporal analysis window as possible and is typically determined by the highest usable frequency in the input seismic data. Near-vertical structural features, such as faults, are enhanced well when using a longer temporal analysis window. By using this algorithm, one would be able to balance the conflicting requirements between maximizing lateral resolution and the increasing signal-to-noise ratio.

Eigenstructure coherency algorithm

The eigenstructure coherency algorithm was presented by Gresztenkorn and Marfurt (1999). This algorithm is based on the determination of seismic trace continuity using a covariance matrix. One definition of the eigenstructure-based coherence estimation makes use of the numerical trace of the covariance matrix \mathbf{C} , denoted by $\text{Tr}(\mathbf{C})$ (Golub and Van Loan, 1989). The numerical trace of \mathbf{C} may be expressed in terms of the matrix \mathbf{D} , the matrix \mathbf{C} , or the eigenvalues of \mathbf{C} . The matrix \mathbf{D} , which represents a multi-channel time series, is a mathematical description of the data enclosed by the analysis cube.

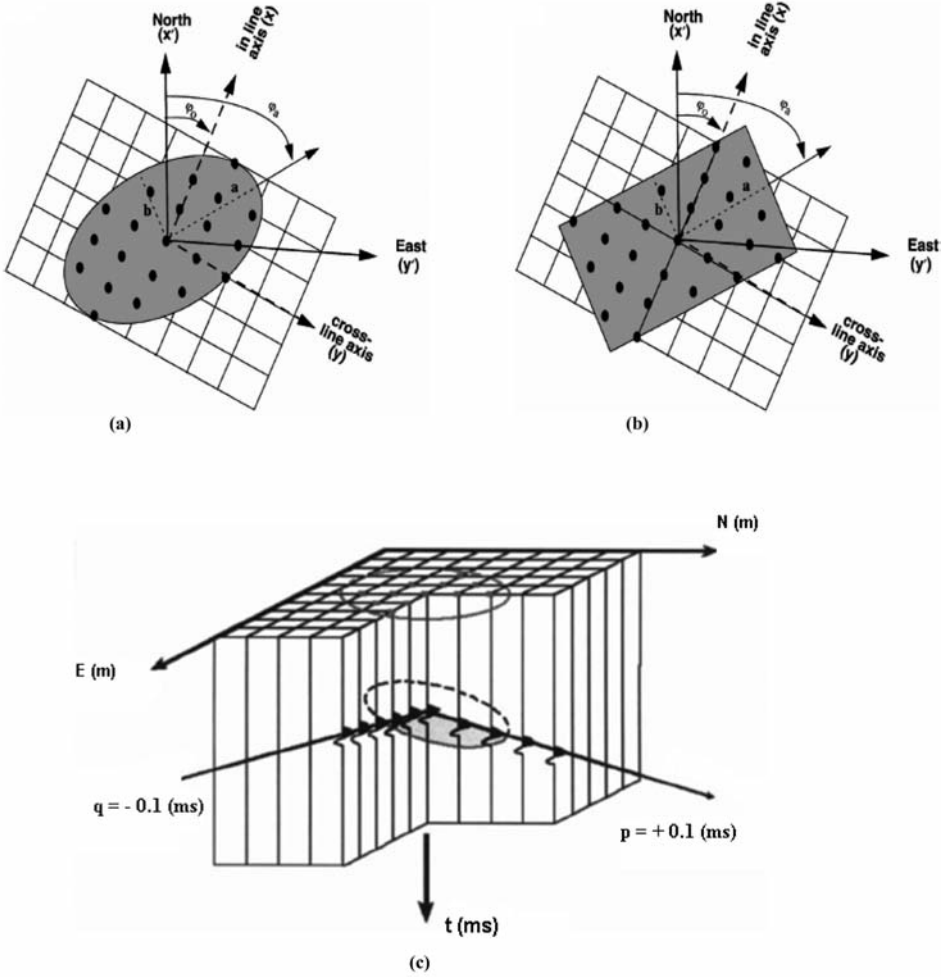


Fig. 1. (a) Elliptical and (b) rectangular analysis windows centered around an analysis point defined by the length of major axis a , the length the of minor axis b , and the azimuth of the major axis φ_a , (c) the calculation of coherency over an elliptical analysis window with apparent dips $(p, q) = (0.1 \text{ ms/m}, -0.1 \text{ ms/m})$ (Marfurt et al., 1998).

A single column of \mathbf{D} represents the N samples of a single trace j whereas a single row of \mathbf{D} denotes the same time sample n common to all J traces. The single entry d_{nj} is therefore the amplitude of the n -th sample of the j -th trace (Gresztenkorn and Marfurt, 1999):

$$\text{Tr}(\mathbf{C}) = \sum_{j=1}^J \sum_{n=1}^N d_{nj}^2 = \sum_{j=1}^J c_{jj} = \sum_{j=1}^J \lambda_j, \quad (3)$$

where J is the number of rows (traces), N shows the number of columns (samples), and λ_j shows eigenvalues.

Fig. 2 shows the comparison between the cross-correlation, semblance and eigenstructure algorithms in detecting micro-faults. Panel (a) shows the vertical seismic section from a 3D seismic cube (in the in-line direction). From this figure it is concluded that the semblance algorithm is superior to the other two algorithms in detecting micro-faults; therefore, the remainder of the study focused on establishing effective parameters only for the semblance algorithm. It should be mentioned that the running time for the cross-correlation, eigenstructure and semblance algorithms were compared in this study. It was considered that the semblance algorithm takes much more time than the cross-correlation and much less time than the eigenstructure algorithms.

EFFECTIVE PARAMETERS ANALYSIS ON THE SEMBLANCE ATTRIBUTE

Among three algorithms related to the coherency attribute, the semblance algorithm is chosen since it can acceptably detect micro-faults in both horizontal and dipping layers. In this section, the dependency of semblance coherency attribute on seismic wavelet dominant frequency, signal-to-noise ratio, analysis window dimensions, and the p and q parameters is analyzed and the optimum values are defined. It is assumed that the seismic wavelet is a time-independent zero-phase Ricker wavelet. Two synthetic models have been used to test the algorithm (Hashemi Gazar and Javaherian, 2008). The first model uses 3D seismic data with dimensions of $300 \times 50 \times 50$ (300 ms time interval), 50 in-lines and 50 x-lines (Fig. 3a). The sampling interval of the first model is 4 ms and the seismic wavelet is a 30 Hz Ricker. There are two normal micro-faults, a and b , generated by a 4 ms shift in time samples. The second model uses 3D seismic data with dimensions of $200 \times 100 \times 100$, a time interval of 200 ms, and 100 in-line and 100 x-line traces (Fig 3b). Three dipping layers are assumed in this model. The sampling interval of the second model is 4 ms and the seismic wavelet is a 35 Hz Ricker. Two micro-faults are generated by a 4 ms shift in the time samples.

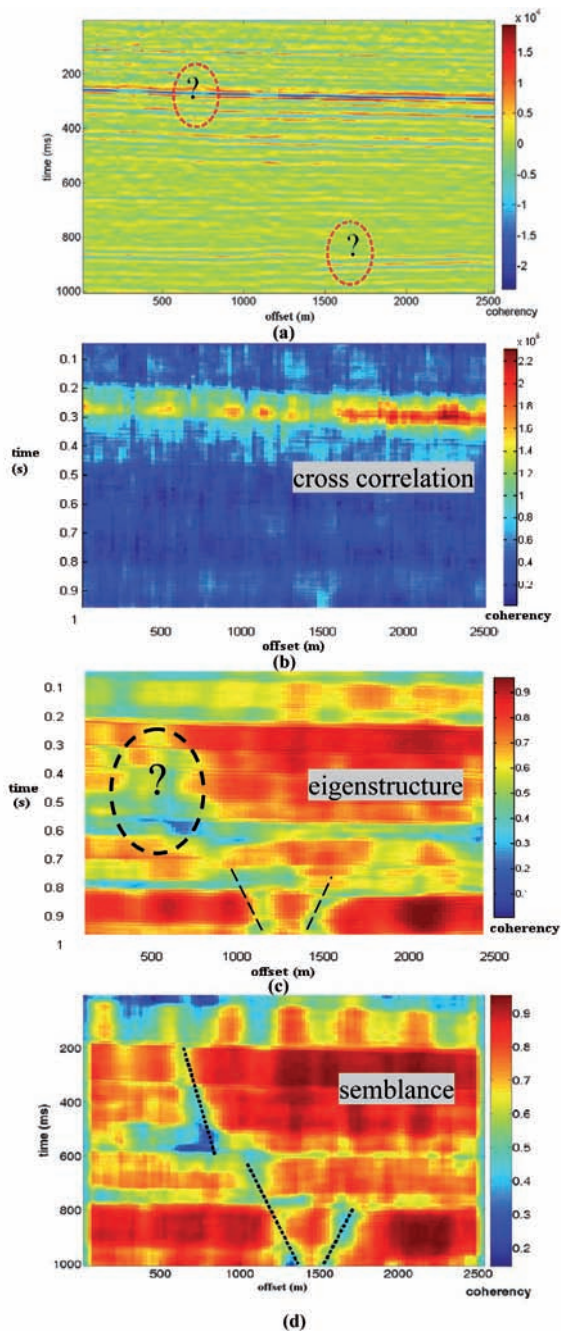


Fig. 2. Comparison among cross-correlation, eigenstructure and semblance coherency algorithms to detect micro-faults. (a) An in-line section from 3D real data, coherency measured by (b) cross-correlation, (c) eigenstructure, and (d) semblance; it can be concluded that the semblance can detect micro-faults better than other two coherency attributes (panels (b) and (c) are from Javaheri Niestanak et al., 2008).

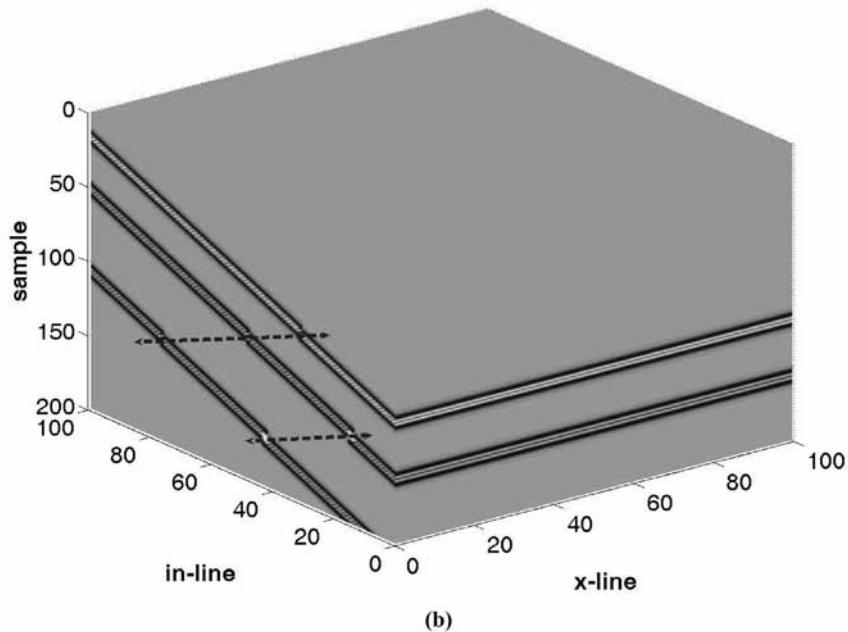
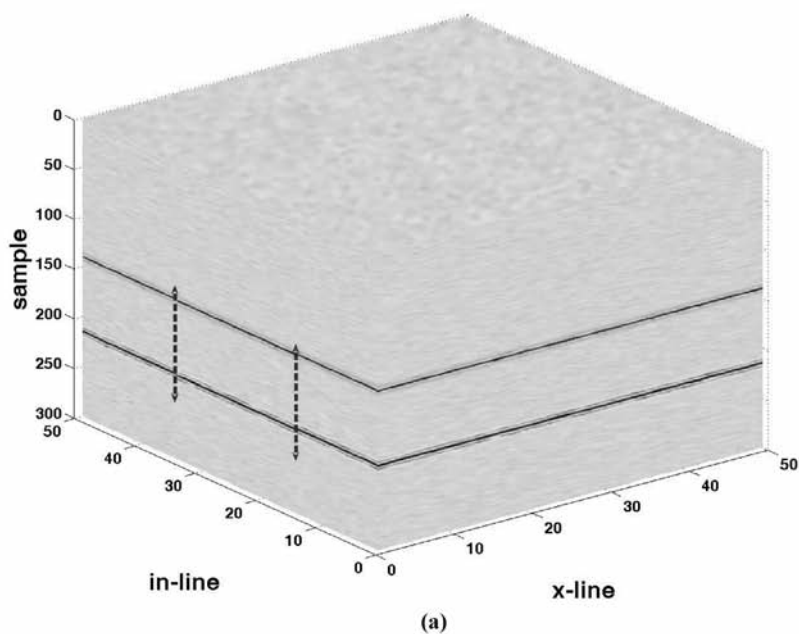


Fig. 3. 3D synthetic seismic cubes with dimensions of (a) $300 \times 50 \times 50$ with two horizontal layers and two micro-fault planes and (b) $200 \times 100 \times 100$ with three dipping layers and two micro-fault planes.

Dominant frequency

Various dominant frequencies of the seismic wavelet are applied to find the differences. For frequencies up to 20 Hz, there is no clear image of the micro-faults. However, for frequencies above 20 Hz, the resolution of micro-faults will increase. By increasing the dominant frequency from 20 to 40 Hz, the data resolution improves. Increasing the dominant frequency causes an increase in differential color between the area of the micro-faults position and other areas of layers. In addition, layers show in normal thickness. For horizontal layers a dominant frequency of 30 Hz is satisfactory, and for dipping layers a dominant frequency of 35 Hz. One of the advantages of semblance algorithm is its ability to detect micro-faults in a lower dominant frequency situation. This accuracy cannot be obtained using the cross-correlation algorithm.

Signal-to-noise ratio

In order to investigate the effect of signal-to-noise ratio in the efficiency of the algorithm, the signal-to-noise ratio of 0.5, 1, 2, and 3 have been tested. Signal-to noise-ratio is calculated using the following equation (Teleford et al 1976)

$$\text{SNR} = P_{\text{signal}}/P_{\text{noise}} = (A_{\text{signal}}/A_{\text{noise}})^2 , \quad (4)$$

where SNR is the signal-to-noise ratio, P is the power and A is the amplitude. Results introduce signal-to-noise ratio as an effective parameter in the performance analysis of the semblance algorithm. Micro-faults are detectable with a signal-to-noise ratio of 1 or higher. When the signal-to-noise ratio of 0.5 is selected, micro-faults can be detectable but with a lower resolution. By increasing the signal-to-noise ratio to 2, high resolution detection will be possible. Models illustrated in Fig. 3 have been applied to the semblance algorithm. The algorithm is able to detect micro-faults in a low signal-to-noise ratio. Apparently, by increasing the signal-to-noise ratio, results can be seen in higher resolutions.

Analysis cube dimensions

One of the parameters that seems to be the most effective in enhancing the performance of the semblance coherency attribute is the dimensions of the analysis cube. To find the best size, several dimensions were applied to the algorithm. First, the optimum analysis cube dimensions for the horizontal layers model were determined. Then, a similar procedure was applied to the dipping

layers model. Figs. 4 and 5 show the efficacy of temporal window on the coherency seismic attribute for the seismic cubes of Fig. 3. As shown, by increasing the k value (i.e. the length of the temporal window in the vertical direction), the vertical resolution is increased. Generally, a vertical analysis window (temporal) is used to detect micro-faults and to improve signal-to-noise ratio. By increasing the vertical-correlation window for the highly dipping layers and normal micro-faults, the signal-to-noise ratio increases but the lateral clearness decreases and the thickness of layers is exaggerated. Horizontal-analysis window (spatial) is used to balance the lateral resolution against the signal-to-noise ratio. By increasing the number of traces, the time of calculation increases naturally. Increasing the number of traces leads to signal-to-noise ratio improvement (Marfurt et al 1998). According to the results, the best k values are 5, 8 and 12, and by going from 5 to 12, the vertical resolution increases (Figs. 4 and 5). For the assumed models here, a k value of 8 for horizontal and dipping layers shows good results (Figs. 4c and 5c). The best spatial window is 10×10 , and after that 10×5 . Therefore, the optimum cube dimensions of analysis are $10 \times 10 \times 8$, which is shown in Figs. 4c and 5c. For these dimensions, the signal-to-noise ratio increases and micro-faults are clearly detectable.

In this method, we are unable to use signal frequency for defining the window width. That is because if we have a low frequency in data by increasing window width we lose lateral resolution even though we may achieve a higher signal-to-noise ratio. Increasing the time-window width increases the signal-to-noise ratio but decreases the lateral resolution and the thickness of layers is exaggerated. Therefore, the time-window could not mainly estimated by the dominant frequency of the signal.

p and q parameters

The values of p and q (i.e., apparent dip in x - and y -directions, respectively, in ms/m) should be effective in the performance of the algorithm. The efficacy of these parameters was studied to detect micro-faults over the cross-dipping layer model. Fig. 6a shows the synthetic seismic cube including two cross-dipping layers with the dimensions of $200 \times 100 \times 100$. The time sampling interval is 4 ms. The dominant frequency is 35 Hz and the signal-to-noise ratio is 1. In order to find the optimum values for p and q , several values were applied. With analysis cube dimensions of $10 \times 10 \times 5$, as shown in Fig. 6b, the algorithm could detect the micro-faults, but the coherency value is high. The high value of the coherency in the micro-faults is incorrect. Therefore, it is necessary to add p and q parameters to the algorithm. In Figs. 6c and 6d, the location of the micro-faults and coherency values are estimated correctly. The optimum value of the parameters for this model is 10 ms/m for both p and q .

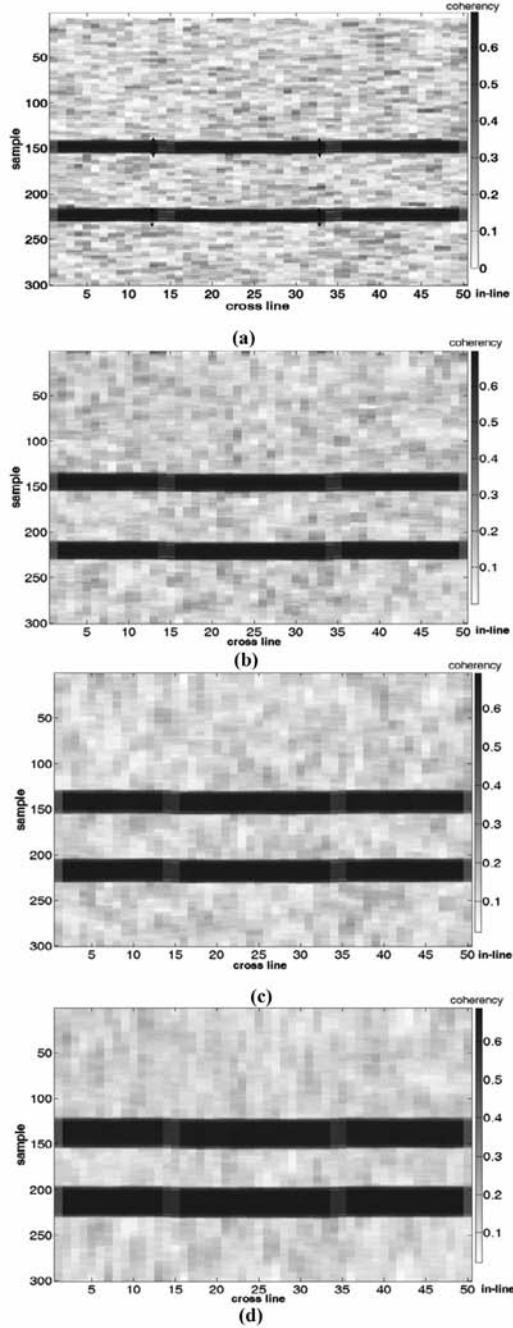


Fig. 4. Semblance attribute of the in-line section of Fig. 3a, showing the effect of the temporal-window length (k) on this attribute. In this analysis, the signal-to-noise ratio is 1 with the dominant frequency of 35 Hz and a spatial window of 10×10 , where for (a) $k = 2$, (b) $k = 5$, (c) $k = 8$, and (d) $k = 12$. Increasing the temporal-window length causes the vertical resolution to increase. For this data, $k = 8$ seems better than the others.

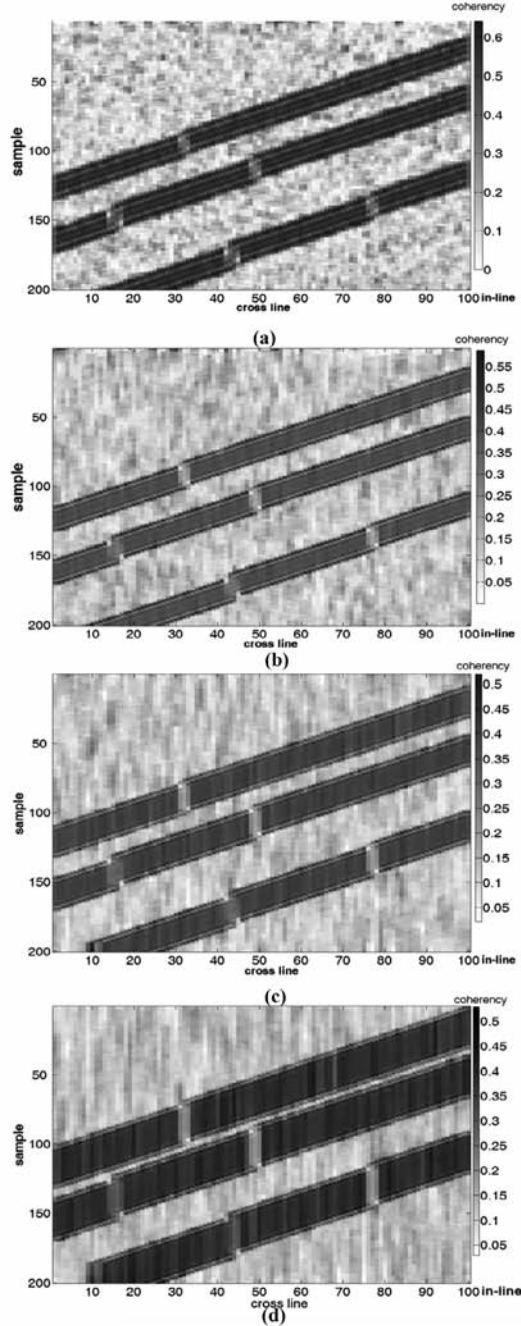


Fig. 5. Semblance attribute of the in-line section of Fig. 3b, showing the effect of the temporal-window length (k) on this attribute. In this analysis, the signal-to-noise ratio is 1 with the dominant frequency of 35 Hz and a spatial window of 10×10 , where for (a) $k = 2$, (b) $k = 5$, (c) $k = 8$, and (d) $k = 12$. Increasing the temporal-window length causes the vertical resolution to increase. For this data, $k = 8$ seems better than the others.

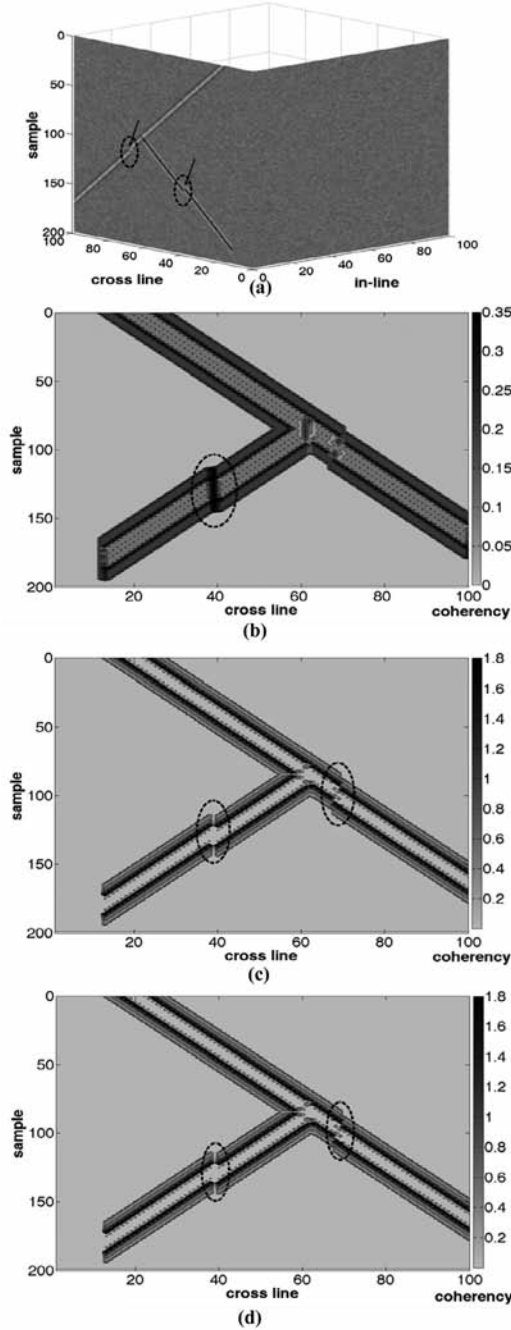


Fig. 6. (a) A 3D synthetic seismic cube with dimensions of $200 \times 100 \times 100$ contains two cross-dipping layers with micro-fault planes; (b) an analysis cube with dimensions of $10 \times 10 \times 5$, showing that the semblance algorithm detects the positions of micro-faults but the coherency values are incorrect; and analysis cubes with dimensions of (c) $5 \times 10 \times 5$ and (d) $10 \times 10 \times 5$, with p and $q = 10$ ms/m. Ellipses show the semblance algorithm detects the positions of micro-faults.

REAL DATA

In order to investigate the application of the semblance algorithm to real seismic data, both a stacked and a time-migrated cube were used. These cubes are related to one of the gas reservoirs located in northeastern Iran. The time sampling interval was 4 ms. The trace interval was 25 m in both in-line and x-line directions. The migrated cube dimensions were 2525 m in the in-line direction (101 in-lines), 1775 m in the x-line direction (71 x-lines) and 1000 ms in the time direction (Fig. 7). Two time slices, in 848 ms and 260 ms, were selected to examine the resolution ability of the semblance algorithm.

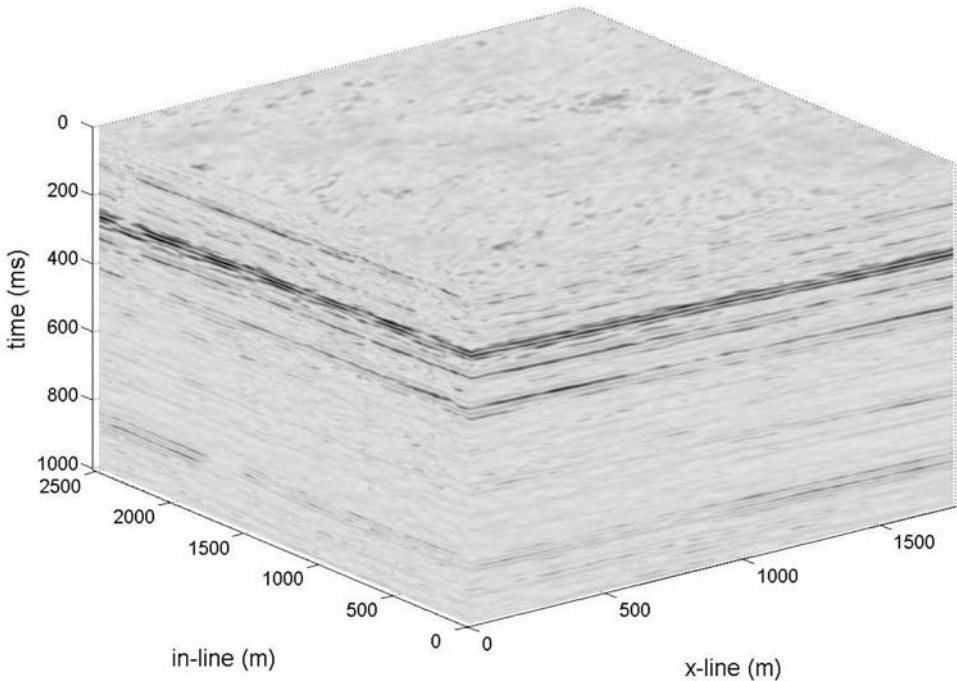


Fig. 7. A 3D seismic cube from one of the oil fields situated in the northeast of Iran. The size of data is 2525 m in the in-line direction and 1775 m in the x-line direction with 1 sec depth length. the trace interval is 25 m, and the sample interval is 4 ms.

Fig. 8 shows the efficacy of the coherency attribute to detect micro-faults in the time slice of 848 ms from Fig. 7 using analysis cubes of (a) $16 \times 5 \times 5$, (b) $16 \times 10 \times 5$, (c) $12 \times 15 \times 10$ and (d) $12 \times 15 \times 15$ dimensions. Micro-fault positions in panels (c) and (d) are identified better than in panels (a) and (b). By

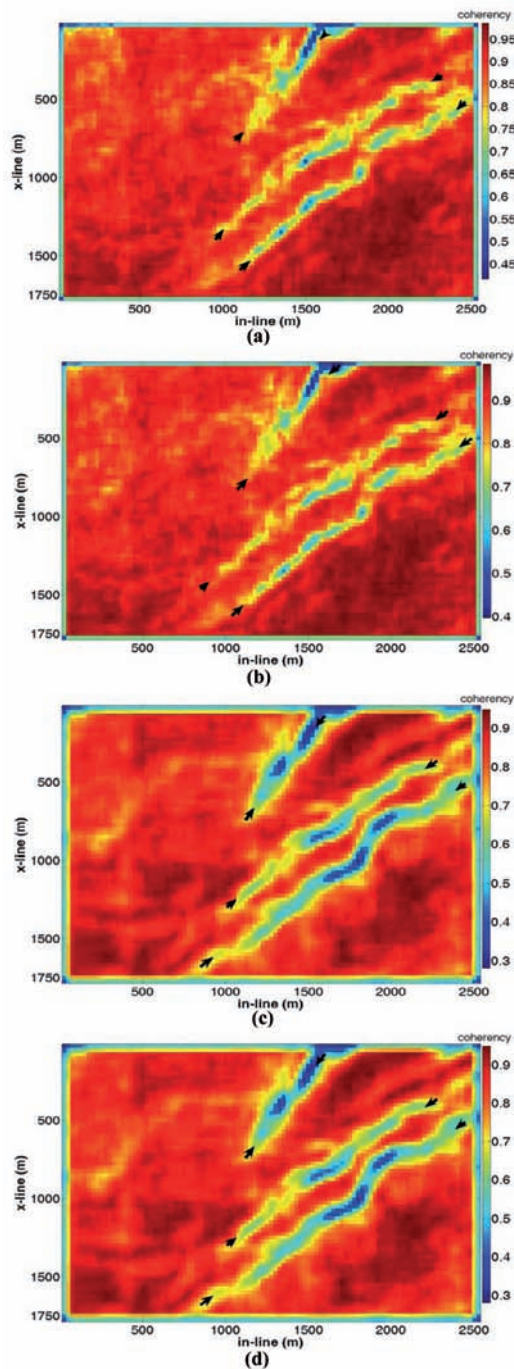


Fig. 8. Efficacy of the coherency attribute in detecting micro-faults in the time slice of 848 ms from Fig. 12 by analysis of cubes with dimensions of (a) $16 \times 5 \times 5$, (b) $16 \times 10 \times 5$, (c) $12 \times 15 \times 10$, and (d) $12 \times 15 \times 15$. The micro-fault positions in panels (c) and (d) are identified better than those in panels (a) and (b).

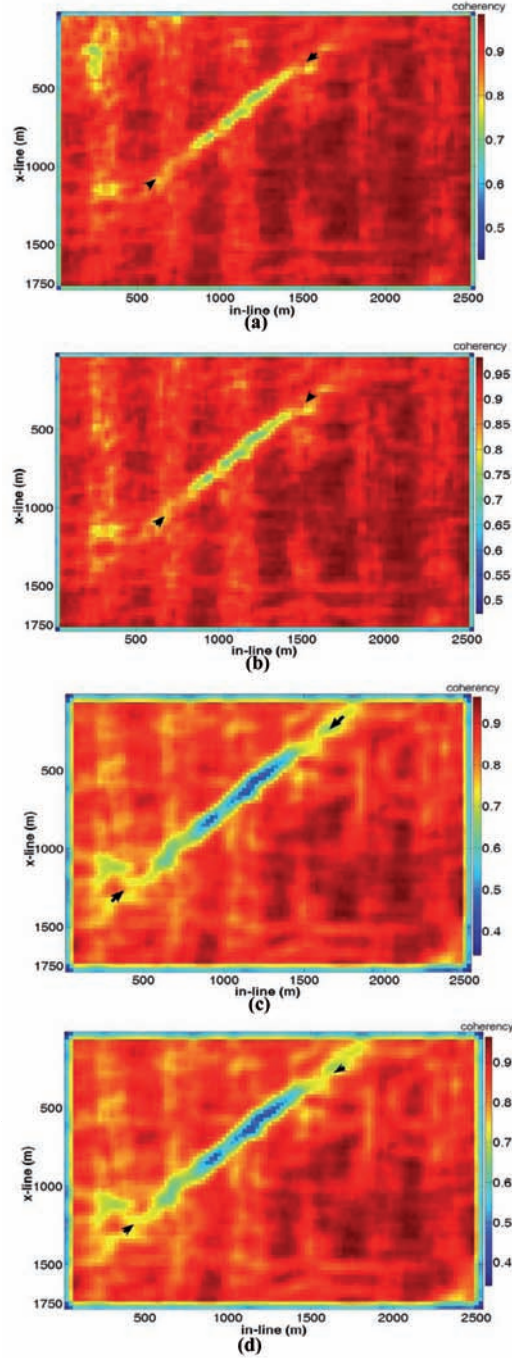


Fig. 9. Efficacy of the coherency attribute in detecting micro-faults in the time slice of 260 ms from Fig. 7 by analysis of cubes with dimensions of (a) $16 \times 5 \times 5$, (b) $16 \times 10 \times 5$, (c) $12 \times 15 \times 10$, and (d) $12 \times 15 \times 15$. The micro-fault positions in panels (c) and (d) are identified better than those in panels (a) and (b).

increasing the analysis window dimensions from 5×5 and 10×5 to 15×10 and 15×15 , resolution of the images improved as shown in Figs. 8c and 8d. When the dimensions of the analysis window exceed 15×15 , no further improvement was observed and the computation time for running the algorithm increased significantly. From this figure, it can be concluded that by increasing the analysis cube dimensions, micro-faults are shown more clearly and the important factor in improving the horizontal resolution is the lateral window dimensions. It was found that the optimum dimensions of the analysis cube for the real data are $12 \times 15 \times 10$ whose results showed the micro-faults in the clearest quality and obviously had less running time in comparison with the $12 \times 15 \times 15$ cube. Fig. 9 shows the ability of the coherency seismic attribute in detecting micro-faults in a time slice of 260 ms. In Figs. 9a and 9b, the algorithm could detect the micro-faults but had poor resolution. By increasing the analysis window dimensions, the resolution of the images improved, as shown in Figs. 9c and 9d. This higher resolution could improve the interpretation of seismic sections.

Fig. 10 shows the sections extracted from the seismic cube in Fig. 7 in in-line and in x-line directions, in which micro-faults are not clear. After applying the semblance algorithm, more information could be extracted. Fig. 11 shows the results of applying the method to the seismic section of Fig. 10a. Four analysis cube dimensions of (a) $16 \times 5 \times 5$, (b) $16 \times 10 \times 5$, (c) $12 \times 15 \times 5$, and (d) $12 \times 15 \times 10$ were used. The results are more convincing in a cube with dimensions of $16 \times 5 \times 5$ (Fig. 11a) as compared with $16 \times 10 \times 5$ (Fig. 11b). Outcomes of the algorithm in two analysis cubes with dimensions of $12 \times 15 \times 5$ and $12 \times 15 \times 10$ are presented in Figs. 11c and 11d. In comparison with Figs. 11a and 11b, micro-faults are clearer in Figs. 11c and 11d. Fig. 12 shows the ability of the algorithm in the seismic section of Fig. 10b. Four analysis cube dimensions of (a) $20 \times 5 \times 5$, (b) $20 \times 15 \times 5$, (c) $12 \times 15 \times 5$, and (d) $12 \times 15 \times 10$ were used. In comparison with Figs. 12a and 12b, micro-faults are clearer in Figs. 12c and 12d.

DISCUSSION

Seismic interpreters use different tools to improve the interpretation of seismic data. Employment of coherency algorithms may be useful at all levels of interpretation. Detection of small-scale discontinuities such as micro-faults can be difficult or even impossible. However, by using coherency algorithms, particularly the semblance-based one, this aim is feasible. The quality of the images depends on input data quality. If the input data has a high noise level, considering the goal, the dimensions of the analysis cube can be modified until the best result is obtained. Near-vertical structural features, such as micro-faults are better enhanced when using a longer temporal analysis window. With this algorithm, it is possible to balance the conflicting requirements of maximizing the lateral resolution and increasing the signal-to-noise ratio.

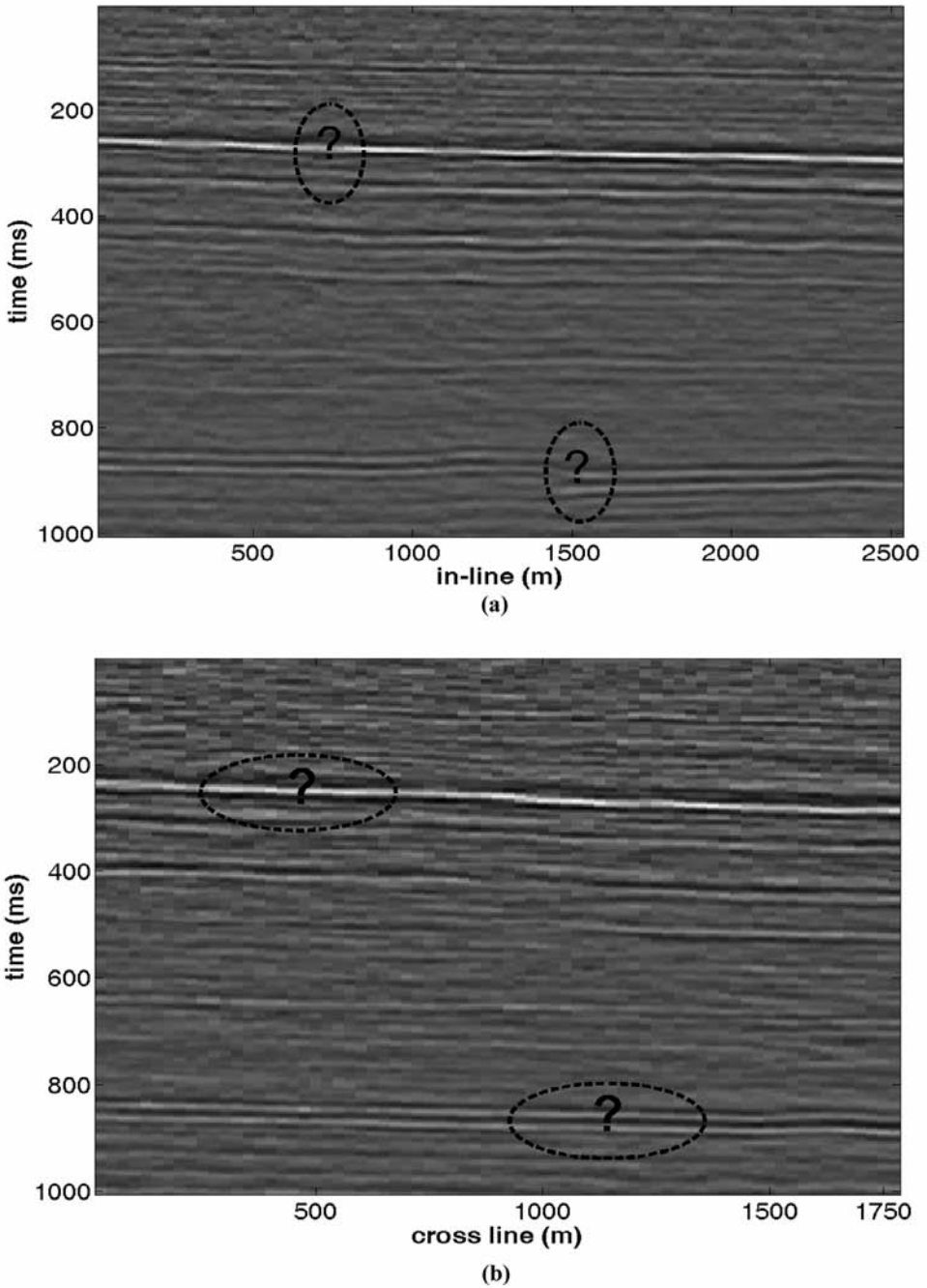


Fig. 10. A vertical seismic section from the 3D seismic cube of Fig. 9, showing (a) the in-line direction and (b) the x-line direction. As can be seen, the micro-fault positions are not assigned in ellipses.

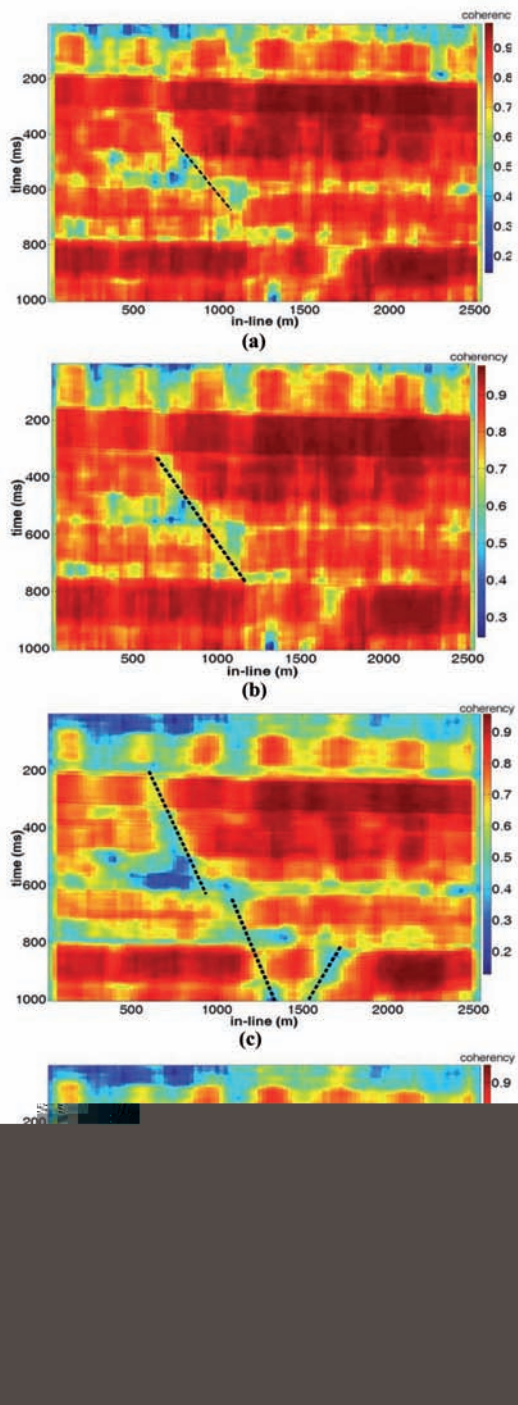


Fig. 11. Efficacy of coherence attributes in detecting micro-faults in Fig. 10a. Analysis cubes are: (a) $16 \times 5 \times 5$, (b) $16 \times 10 \times 5$, (c) $12 \times 15 \times 5$ and (d) $12 \times 15 \times 10$. Arrows show the micro-faults. Microfault positions in panels (c) and (d) are identified better than those in panels (a) and (b).

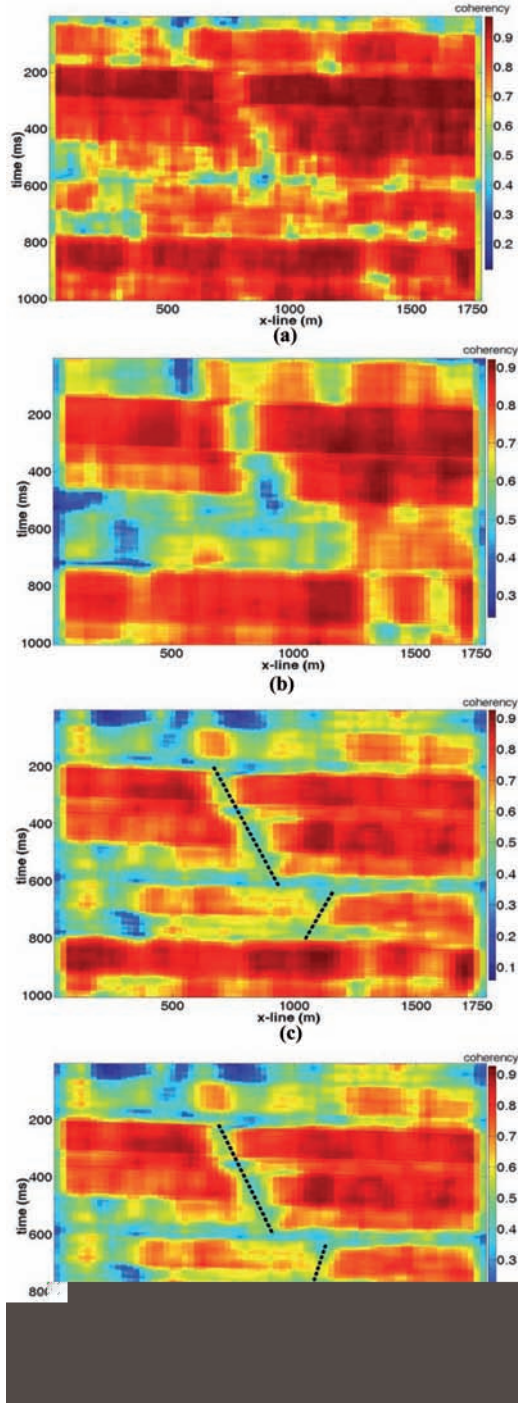


Fig. 12. Efficacy of coherence attributes in detecting minor micro-faults in Fig. 10b. Analysis cubes are (a) $20 \times 5 \times 5$, (b) $20 \times 15 \times 5$, (c) $12 \times 15 \times 5$, and (d) $12 \times 15 \times 10$. Arrows show the micro-faults. Micro-fault positions in panels (c) and (d) are identified better than those in panels (a) and (b).

CONCLUSIONS

Coherency attributes can help interpreters in the interpretation of seismic data. These attributes are sensitive to several parameters, such as the dominant frequency of seismic wavelet, the signal-to-noise ratio, and the dimensions of the analysis cube. In coherency algorithms, by increasing both the dominant frequency of seismic wavelet and the signal-to-noise ratio, the resolution of images is improved. Also, increasing the dominant frequency of seismic wavelet can detect layers in their actual thicknesses and prevent layer widening. Generally, the quality of the images depends on input data quality. If the input data has high noise, considering the goal, the dimensions of the analysis cube can be changed until the best result is obtained. An increase in the spatial window of the dimensions of the analysis cube will lead to an increase in the signal-to-noise ratio and a decrease in the lateral resolution. Therefore, the optimum dimensions should be obtained. The length of the time window affects the signal-to-noise ratio. Changing this parameter is useful in the detection of thin layers. Analyses show that semblance is better than cross-correlation or eigenstructure algorithms in detecting micro-faults.

In this study, several parameters of the semblance algorithm are analyzed and some parameters are defined. The results indicate that micro-faults are detectable with a signal-to-noise of 1 or higher. When a signal-to-noise ratio of 0.5 is selected, micro-faults can be detectable but with a lower resolution. For frequencies up to 20 Hz, there is no clear image of the micro-faults, but for frequencies above 20 Hz, resolution of micro-faults will increase. The size of temporal window of 32 ms ($k = 8$) for horizontal and dipping layers shows good results. The best size for the spatial window is 10×10 , and after that 10×5 . Therefore, the optimum cube dimensions of analysis are $10 \times 10 \times 8$. For these dimensions, the signal-to-noise ratio increases and micro-faults are clearly detectable. For cross-dipping layers it is necessary to add p and q parameters to the algorithm because the location of the micro-faults and coherency value are estimated correctly. The optimum value of the parameters is 10 ms/m for both p and q . In the case of dipping layers, p and q parameters are effective in the semblance-based algorithm results. The real data used in this study is related to carbonate units and resulted in a satisfactory performance. Micro-faults and minor fractures hidden the primary data were detectable after applying the algorithm.

REFERENCES

- Al-Dossary, S. and Marfurt, K.J., 2006. Multispectral estimates of reflector curvature and rotation. *Geophysics*, 71: P41-P51.
- Bahorich, M.S. and Farmer, S.L., 1995. 3-D seismic discontinuity for faults and stratigraphic features; the coherence cube. *The Leading Edge*, 14: 1053-1058.
- Chopra, S. and Marfurt, K.J., 2005. Seismic attributes - A historical perspective. *Geophysics*, 70: 3SO-28SO.
- Chopra, S. and Marfurt, K.J., 2007a. Multispectral volumetric curvature adding value to 3D seismic data interpretation. Expanded Abstr., CSPG/CSEG Conv., Calgary.
- Chopra, S. and Marfurt, K.J., 2007b. Volumetric curvature attributes for fault/fracture characterization. *First Break*, 25: 35-46.
- Golub, G.H. and Van Loan, C.F., 1989. *Matrix Computations*, 2nd Ed. The Johns Hopkins University, Baltimore.
- Gersztenkorn, A. and Marfurt, K.J., 1996a. Coherence computations with eigenstructure. Extended Abstr., 58th EAGE Conf., Amsterdam: X031.
- Gersztenkorn, A. and Marfurt, K.J., 1996b. Eigenstructure based coherence computations. Expanded Abstr., 66th Ann. Internat. SEG Mtg., Denver: 328-331.
- Gersztenkorn, A. and Marfurt, K.J., 1999. Eigenstructure-based coherence computations as an aid to 3-D structural and stratigraphic mapping. *Geophysics*, 64: 1468-1479.
- Hart, B.S., Pearson, R. and Rawling, G.C., 2002. 3-D seismic horizon-based approaches to fracture-swarm sweet spot definition in tight-gas reservoirs. *The Leading Edge*, 21: 28-35.
- Javaheri Niestanak, A.R., Javaherian, A. and Amini, N., 2008. Fault detection using coherency attribute. *Scientif. Quart. J. Geoscienc.*, 17: 48-59 (in Farsi with abstract in English).
- Marfurt, K.J., Kirlin, R.L., Farmer, S.L. and Bahorich, M.S., 1998. 3-D seismic attributes using a running window semblance-based algorithm. *Geophysics*, 63: 1150-1165.
- Masaferro, J.L., Bulnes, M., Poblet, J. and Casson, M., 2003. Kinematics evolution and fracture prediction of the Valle Morado structure inferred from 3-D seismic data, Salta Province, northwest Argentina. *AAPG Bull.*, 87: 1083-1104.
- Roberts, A., 2001. Curvature attributes and their application to 3-D interpreted horizons. *First Break*, 19: 85-99.
- Rummerfeld, B., 1954. Reflection quality, a fourth dimension. *Geophysics*, 19: 684-694.
- Sigismondi, M. and Soldo, J.C., 2003. Curvature attributes and seismic interpretation: Case studies from Argentina basins. *The Leading Edge*, 22: 1122-1126.
- Taner, M.T., 2001. Seismic attributes. *CSEG Recorder*, 26: 49-55.
- Teleford, W.M., Geldrat, L.P., Sheriff, R.E. and Keys, D.A., 1976. *Applied Geophysics*. Cambridge University Press, Cambridge.